# Catalytic Mechanism of Guanidinoacetate Methyltransferase: Crystal Structures of Guanidinoacetate Methyltransferase Ternary Complexes[†,‡]

Junichi Komoto,[§] Taro Yamada,[§] Yoshimi Takata,[§,||] Kiyoshi Konishi,[||,⊥] Hirofumi Ogawa,[||] Tomoharu Gomi,[||] Motoji Fujioka,[||,@] and Fusao Takusagawa*[,§]

*Department of Molecular Biosciences, University of Kansas, 1200 Sunnyside Avenue, Lawrence, Kansas 66045-7534, and Department of Biochemistry, Faculty of Medicine, Toyama Medical and Pharmaceutical University, Sugitani, Toyama 930-01, Japan*

*Received June 24, 2004; Revised Manuscript Received September 3, 2004*

ABSTRACT: Guanidinoacetate methyltransferase (GAMT) is the enzyme that catalyzes the last step of creatine biosynthesis. The enzyme is found in abundance in the livers of all vertebrates. The intact GAMT from recombinant rat liver has been crystallized with an inhibitor *S*-adenosylhomocysteine (SAH) and a substrate guanidinoacetate (GAA), and with SAH and an inhibitor guanidine (GUN). These ternary complex structures have been determined at 2.0 Å resolution. GAMT has an $\alpha/\beta$ open-sandwich structure, and the N-terminal section (residues 1−42) covers the active site entrance so that the active site is not visible. SAH has extensive interactions with GAMT through H-bonds and hydrophobic interactions. The guanidino groups of GAA and GUN form two pairs of H-bonds with E45 and D134, respectively. The carboxylate group of GAA interacts with the backbone amide groups of L170 and T171. A model structure of GAMT containing the two substrates (SAM and GAA) was built by attaching a methyl group ($C_E$) on $S_D$ of the bound SAH. On the basis of this model structure, a catalytic mechanism of GAMT is proposed. The active site entrance is opened when the N-terminal section is moved out. GAA and SAM enter the active site and interact with the amino acid residues on the surface of the active site by polar and nonpolar interactions. $O_{D1}$ of D134 and $C_E$ of SAM approach $N_E$ of GAA from the tetrahedral directions. The $O_{D1}\cdots N_E$ and $C_E\cdots N_E$ distances are 2.9 and 2.2 Å, respectively. It is proposed that three slightly negatively charged carbonyl oxygen atoms (O of T135, O of C168, and $O_B$ of GAA) around $O_{D1}$ of D134 increase the p$K_a$ of $O_{D1}$ so that $O_{D1}$ abstracts the proton on $N_E$. A strong nucleophile is generated on the deprotonated $N_E$ of GAA, which abstracts the methyl group ($C_E$) from the positively charged $S_D$ of SAM, and creatine (methyl-GAA) and SAH (demethyl-SAM) are produced. E45, D134, and Y221 mutagenesis studies support the proposed mechanism. A mutagenesis study and the inhibitory mechanism of guanidine analogues support the proposed mechanism.

Guanidinoacetate methyltransferase (*S*-adenosyl-L-methionine:guanidinoacetate *N*-methyltransferase, GAMT,[1] EC 2.1.1.2), first found in pig liver by Cantoni and Vignos, is the enzyme that catalyzes the last step of creatine biosynthesis (*1*). The enzyme is found in abundance in the livers of all vertebrates.

In humans, the biosynthesis of creatine is reported to represent ∼75% of the total utilization of methionine through

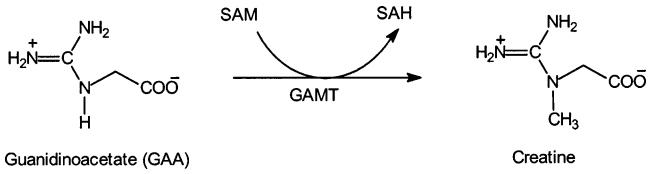


*S*-adenosylmethionine (SAM) (*2*), and thus, GAMT is believed to be the major enzyme involved in the metabolic conversion of SAM to *S*-adenosylhomocysteine (SAH) in vertebrates (*3*). SAH inhibits severely most SAM-dependent methyltransferases, including GAMT (*4*−*8*). A hereditary disease with extrapyramidal motor disorder and extremely low concentrations of creatine in the brain, serum, and urine has recently been described (*9*) and was shown to be due to a deficiency of GAMT in the liver (*10*, *11*). Oral supplementation with 0.35−2.0 g of creatine/kg/day slowly increases the total creatine concentration in the brain (*12*, *13*).

GAMT was purified to homogeneity from the livers of pig and rat by Im *et al.* (*14*) and Ogawa *et al.* (*15*), respectively, and shown to be a monomeric protein with a relatively small molecular size ($M_r$ = 25 800). The amino acid sequences of the rat (*16*) and human enzymes (*17*) were

[†] The work carried out at the University of Kansas has been supported by American Heart Association Grant 0455454Z.

[‡] The atomic coordinates and structure factors have been deposited with the Protein Data Bank (entries 1XCJ and 1XCL).

* To whom all correspondence should be addressed: Department of Molecular Biosciences, University of Kansas, 1200 Sunnyside Ave., Lawrence, KS 66045-7534. Telephone: (785) 864-4727. Fax: (785) 864-5321. E-mail: xraymain@ku.edu.

[§] University of Kansas.

[||] Toyama Medical and Pharmaceutical University.

[⊥] Present address: Department of Microbiology, The Nippon Dental University, 1-9-20 Fujimi, Chiyoda-ku, Tokyo 102, Japan.

[@] Deceased May 15, 2004.

[1] Abbreviations: GAA, guanidinoacetate; GAMT, guanidinoacetate methyltransferase; GUN, guanidine; Hcy, homocysteine; SAH, *S*-adenosyl-L-homocysteine; SAM, *S*-adenosyl-L-methionine; WT, wild-type enzyme (GAMT).

10.1021/bi0486785 CCC: $27.50 
Published on Web 10/23/2004

deduced from the respective cDNA sequences. Between the two enzymes, there is 82.5% homology in the nucleotide sequence and 86.9% homology in the amino acid sequence. Rat liver GAMT was produced recombinantly in large amounts in *Escherichia coli* (*16*), and its structural and functional features have been studied by chemical modification, site-directed mutagenesis, and limited proteolysis (*18*−*23*). The 36 amino acid residues at the N-terminus of rat liver GAMT were cleaved during the purification, and the crystal structure of the truncated enzyme was determined at 2.5 Å resolution (*24*, *25*). The truncated enzyme forms a dimer, and each subunit contains one SAH molecule in the active site. R220[2] of the partner subunit enters deeply into the active site and forms a pair of H-bonds with D134. The dimer structure of the truncated GAMT looks like a protein arginine methyltransferase (one of the subunits) that forms a complex with a target protein (the other subunit). Since the N-terminally truncated GAMT shows a very weak protein arginine methyltransferase activity, the dimer structure of the truncated enzyme has provided a model structure of protein arginine methyltransferases (*24*).

A secondary structure prediction by the PSA server (*26*) suggested that the truncated N-terminal section would form a long α-helix (residues 10−27) and a *β*-strand (residues 31−35). A ternary complex structure of the intact GAMT was built on the basis of the N-terminally truncated structure and the secondary structure prediction, and a possible catalytic mechanism was proposed (*24*). In the model, GAA[3] binds to the active site in a manner similar to that of R220 and the carboxylate group of GAA forms a pair of H-bonds with R20. However, later, we found that the R20A mutation did not affect the catalytic activity (unpublished data), indicating that an intact GAMT model structure and the proposed mechanism had some problems.

Here we present the crystal structures of intact GAMT ternary complexes [GAMT−(SAH + GAA) and GAMT−(SAH + GUN)]. On the basis of these ternary complex structures, we propose a catalytic mechanism of the methyl transfer reaction by GAMT. A mutagenesis study and the inhibitory mechanism of guanidine analogues support the proposed mechanism.

## MATERIALS AND METHODS

*Purification and Crystallization Procedures.* GAMT used in this study is the recombinant rat enzyme produced in *E. coli* JM109 transformed with the pUCGAT9-1 plasmid that contains the coding sequence of rat GAMT cDNA (*16*). The enzyme was purified to homogeneity from *E. coli* extracts by gel filtration over Sephacryl S-200 and DEAE-cellulose chromatography as described previously (*27*). A cocktail of protease inhibitors (from Sigma) was used to prevent proteolysis, and the intact enzyme was purified. Recombinant GAMT lacks the N-terminal acetyl group but exhibits kinetic parameters similar to those of the liver enzyme (*15*, *16*).

The hanging-drop vapor-diffusion method was employed for crystallization of the enzyme. The initial crystallization condition was found by a crystallization screening procedure. Crystals of GAMT−(SAH + GAA) were grown in a solution containing 8 mg/mL GAMT, 1 mM SAH, 2 mM GAA, 0.25 M sodium chloride, 5 mM tris(carboxyethyl)phosphine (TCEP), 24−26% PEG 8000, and 50 mM MES buffer (pH 6.0) in a 4 °C cold room. Prismatic crystals suitable for X-ray diffraction studies (∼0.20 mm × 0.15 mm × 0.15 mm) were grown in 2 weeks. Crystals containing SAH and guanidine (GUN) [GAMT−(SAH + GUN)] were grown in a solution containing 10 mg/mL GAMT, 2 mM SAH, 10 mM guanidine hydrochloride, 0.1 M sodium acetate, 5 mM TCEP, 20−28% PEG 8000, and 50 mM MES buffer (pH 6.5) in a 4 °C cold room. Prismatic crystals suitable for X-ray diffraction studies (∼0.20 mm × 0.15 mm × 0.15 mm) were grown in 2 weeks.

*Data Measurement.* The crystals of GAMT−(SAH + GAA) and GAMT−(SAH + GUN) in a hanging drop were scooped with a nylon loop and dipped into a cryoprotectant solution for 15 min, respectively, before they were frozen in liquid nitrogen. The cryoprotectant solution was composed of the original mother liquor containing 15% ethylene glycol. The frozen crystals were transferred onto a Rigaku RAXIS IIc imaging plate X-ray diffractometer with a rotating anode X-ray generator as an X-ray source (Cu Kα radiation operated at 50 kV and 100 mA). The X-ray beam was focused to 0.3 mm by confocal optics (Osmic, Inc.). The diffraction data were measured up to 2.0 Å resolution at −180 °C. The data were processed with DENZO and SCALEPACK (*28*). The data statistics are given in Table 1.

*Crystal Structure Determination.* The deduced unit cell dimensions of GAMT−(SAH + GAA) and GAMT−(SAM + GUN) indicate that these crystals are isomorphous to each other. The unit cell dimensions and space group (*P*1) indicate that the unit cell contains one complex. The crystal structure of the GAMT−(SAM + GAA) complex was initially determined by a molecular replacement procedure using the N-terminally truncated GAMT−SAH complex (PDB entry 1KHH). The undefined residues (residues 7−42) in the truncated enzyme were built in $2F_o - F_c$ maps. Residues 1−6 were apparently disordered and were not included in the model. The model was refined by the simulated annealing procedures of X-PLOR (*29*). The $2F_o - F_c$ and $F_o - F_c$ maps showed two large significant residual electron density peaks in the active site (Figure 1). A SAH molecule was built in one of the residual electron density peaks. The other residual electron density peak was assigned to GAA. The model was refined with the simulated annealing procedures of X-PLOR. Other well-defined residual peaks were assigned to water molecules. The complex was refined with all data (no $\sigma$ cutoff) at 2.0 Å resolution.

The structure of GAMT−(SAH + GUN) was determined using the coordinates of GAMT−(SAM + GAA). The $2F_o - F_c$ and $F_o - F_c$ maps showed that two well-defined residual electron density peaks corresponding to SAH and GUN, and SAH and GUN, were fitted into the residual electron density peaks, respectively. The complex structure was refined with the same procedure that was applied to GAMT−(SAM + GAA). The coordinates have been depos-

[2] Amino acid residues are denoted with the single-letter code: A for Ala, D for Asp, E for Glu, H for His, K for Lys, L for Leu, N for Asn, R for Arg, S for Ser, T for Thr, W for Trp, and Y for Tyr.

[3] GAA adopts the same atom nomenclature as arginine in the PDB, and two carboxylate oxygen atoms are named $O_A$ and $O_B$

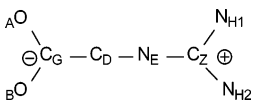

Table 1: Crystallographic Statistics[a]

| | GAMT−(SAH + GAA) | GAMT−(SAH + GUN) |
|---|---|---|
| unit cell | $a = 36.19$ Å, $b = 41.40$ Å, $c = 42.32$ Å, $\alpha = 104.3°$, $\beta = 112.7°$, $\gamma = 104.5°$ | $a = 36.16$ Å, $b = 41.39$ Å, $c = 42.57$ Å, $\alpha = 104.3°$, $\beta = 112.9°$, $\gamma = 104.2°$ |
| resolution (Å) | 2.0 | 2.0 |
| total no. of observations | 68152 | 71975 |
| no. of unique reflections | 12785 | 11808 |
| completeness (%) | 93.4 (73.9) | 85.4 (57.7) |
| $R_{sym}$ (%) (outer shell)[b,c] | 0.038 (0.077) | 0.034 (0.086) |
| no. of protein non-hydrogen atoms | 1816 | 1816 |
| substrate or inhibitor | GAA and SAH | GUN and SAH |
| no. of solvent molecules ($H_2O$) | 60 | 83 |
| resolution range (Å) | 10−2.0 | 10−2.0 |
| total no. of reflections used in $R_{cryst}$ | 11371 | 10493 |
| total no. of reflections used in $R_{free}$ | 1310 | 1208 |
| $R_{cryst}$ (outer shell)[c,d] | 0.225 (0.293) | 0.205 (0.274) |
| $R_{free}$ (outer shell)[c] | 0.279 (0.323) | 0.292 (0.373) |
| rmsd for bond distances (Å) | 0.010 | 0.010 |
| rmsd for bond angles (deg) | 1.4 | 1.4 |
| rmsd for torsion angles (deg) | 22.5 | 22.5 |
| most favored region (%) of the Ramachandran plot | 92.3 | 92.3 |
| additional allowed region (%) of the Ramachandran plot | 7.7 | 7.7 |

[a] $P1$ space group. $M_r = 25\,800$; one complex in the unit cell. $V_M = 2.03$ Å$^3$; 39% solvent content. [b] $R_{sym} = \sum_h\sum_i|I_{hi} - \langle I_h\rangle|/\sum_h\sum_i|I_{hi}|$. [c] Outer shell, 2.0−2.2 Å resolution. [d] $R_{cryst} = \sum|F_o - F_c|/\sum|F_o|$.

ited in the Protein Data Bank (entries 1XCJ and 1XCL, respectively).

*Site-Directed Mutagenesis.* Oligonucleotide-directed mutagenesis was used to prepare cDNAs encoding mutated forms of GAMT. Mutagenic oligonucleotides were purchased from Integrated DNA Technologies (Coraville, IA). Mutagenesis was performed by the method of Kunkel *et al.* (*30*), with a Mutan-K site-directed mutagenesis kit (Takara Shuzo, Kyoto, Japan). A clone containing the desired mutation was identified by nucleotide sequence analysis across the mutation site by the dideoxy chain termination method (*31*).

*Enzyme Assay.* The enzyme catalytic activity of GAMT is measured with coupling reactions with *S*-adenosylhomocysteine hydrolase (SAHH) and adenosine deaminase (ADA) as shown below:

$$\text{GAA} + \text{SAM} \xrightarrow{\text{GAMT}} \text{creatine} + \text{SAH} \xrightarrow{\text{SAHH}} \text{Hcy} + \text{Ado} \xrightarrow{\text{ADA}} \text{inosine} + NH_4^+$$

The GAMT catalytic activities of the WT and mutated enzymes were determined spectrophotometrically, as described in a previous study (*23*).

## RESULTS

*Overall Structure.* The crystallographic refinement parameters (Table 1), final $2F_o - F_c$ maps, and conformational analysis by PROCHECK (*32*) indicate that the structures of GAMT−(SAH + GAA) and GAMT−(SAH + GUN) have been determined with acceptable statistics. Residues 7−42 which were not defined in the truncated GAMT are well-defined in the intact enzyme structure and are folded into a coil−helix(16−19)−coil−strand(25 and 26)−coil−strand-(33−35)−coil−strand(38−42) structure. Residues 1−6 were not defined in the $2F_o - F_c$ maps and are apparently disordered. The core structure (residues 43−235) is essentially the same as that of the N-terminally truncated enzyme and is folded into a typical $\alpha/\beta$-open sandwich structure seen in all known structures of SAM-dependent methyltransferases (Figure 2A). Since the rmsd of $C_A$ positions between GAMT−(SAH + GAA) and GAMT−(SAH + GUN) is 0.1 Å, the structure of GAMT−(SAH + GAA) is mainly described in this paper.

*SAH Binding Site.* As shown in Figure 1, well-defined electron density peaks were observed in the active site of GAMT, indicating that the enzymes contain SAH and GAA, and SAH and GUN, respectively. SAH binds to the C-terminal ends of $\beta_1$ and $\beta_4$, where the strand order is reversed (Figure 2). The adenine ring is in a hydrophobic pocket and forms two H-bonds ($N_3\cdots$N[W116] and $N_6\cdots O_{E1}$[E117]) with GAMT and two H-bonds with a water molecule ($w_5$) connecting $N_6$ and $N_7$ to O of Y136 (Figure 3). The consensus H-bonds connect the 2′-OH and 3′-OH groups of adenosine ribose to acidic amino acid residue E89 located at the C-terminal end of $\beta_2$ (Figures 2 and 3). The 2′-OH and 3′-OH groups also participate in H-bonds with $N_{E1}$[W19] and N[G69], respectively. The carboxyl group of the Hcy moiety is involved in H-bonds with three backbone amide groups (M70, I72, and A73). The amino group of the Hcy moiety participates in H-bonds with $O_{D2}$[D134], $S_D$[M49], and a water molecule ($w_4$). Since D134 forms a pair of H-bonds with the guanidino group of the bound GAA, SAH and GAA are connected through the D134-mediated H-bonds.

Most mammalian non-nucleic acid methyltransferases are monomeric proteins that are rather small in size and share three regions of sequence similarity (motifs I−III from the N-terminal side) (*33*). The sequence of motif I is glycine-rich [oLD(E)oGsGsG, where o and s denote hydrophobic and small neutral amino acid residues, respectively, and $^{63}$VLEVGFGMA$^{71}$ in GAMT]; motif II is characterized by the presence of a conserved aspartate residue that is surrounded by hydrophobic residues (oDso and $^{133}$YDTY$^{136}$ in GAMT) (*34*). Motif III has rather well-defined fingerprint

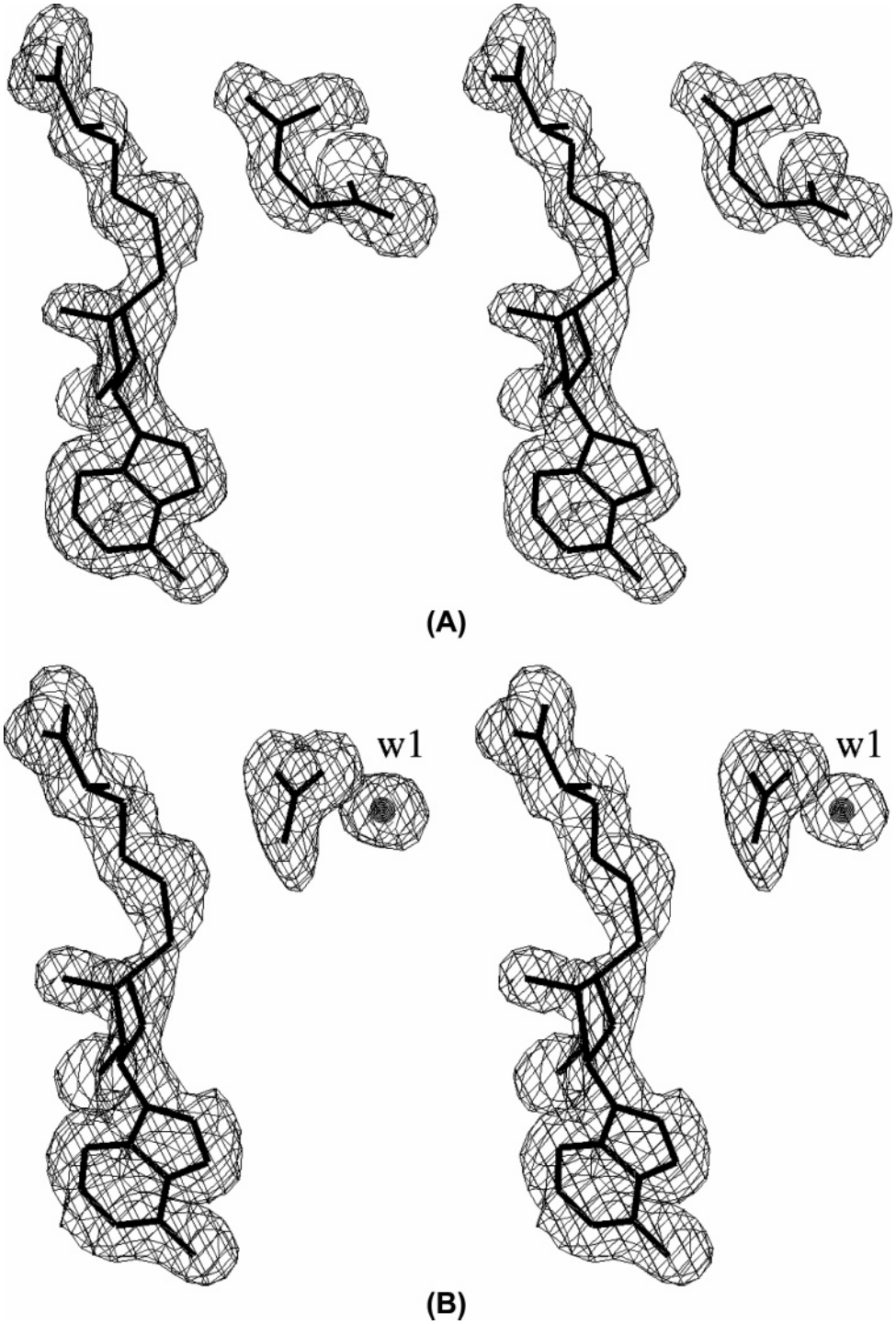


FIGURE 1: $F_o - F_c$ map showing the residual electron density peaks in the active site. The contour is drawn at the 2.5$\sigma$ level: (A) SAH and GAA in GAMT−(SAH + GAA) and (B) SAH, GUN, and a water in GAMT−(SAH + GUN).

residues [LR(K)PGGxL and $^{159}$LKPGGIL$^{165}$ in GAMT] and has no apparent role in substrate binding and catalysis (*35*). The three motifs are always found in the same order on the polypeptide chain and are separated by similar intervals. As shown in Figure 3, motifs I and II are indeed involved in substrate binding and catalysis, which will be discussed below.

*GAA Binding Site.* The substrate GAA is firmly attached to the enzyme by H-bonds (Figure 3A). Each carboxylate group of E45 and D134 forms a pair of H-bonds with the guanidino group of GAA. A water molecule ($w_1$) participates in a bridge H-bond between $N_{H2}$[GAA] and $O_{G1}$[T171]. The carboxylate group of GAA forms a pair of H-bonds with the amide groups of L170 and T171. Also, one of the carboxylate oxygens is involved in two additional H-bonds with $O_{G1}$[T171] and a water molecule ($w_2$). As described above, all polar groups of GAA are involved in H-bonds.

*GUN Binding Site.* GUN binds at the same site of the guanidino group of GAA (Figure 3B). Two water molecules ($w_1$ and $w_2$) bind at the same sites as observed in GAMT−(SAH + GAA). In addition to these water molecules, two water molecules ($w_a$ and $w_b$) occupy the $O_A$ and $O_B$ carbonyl

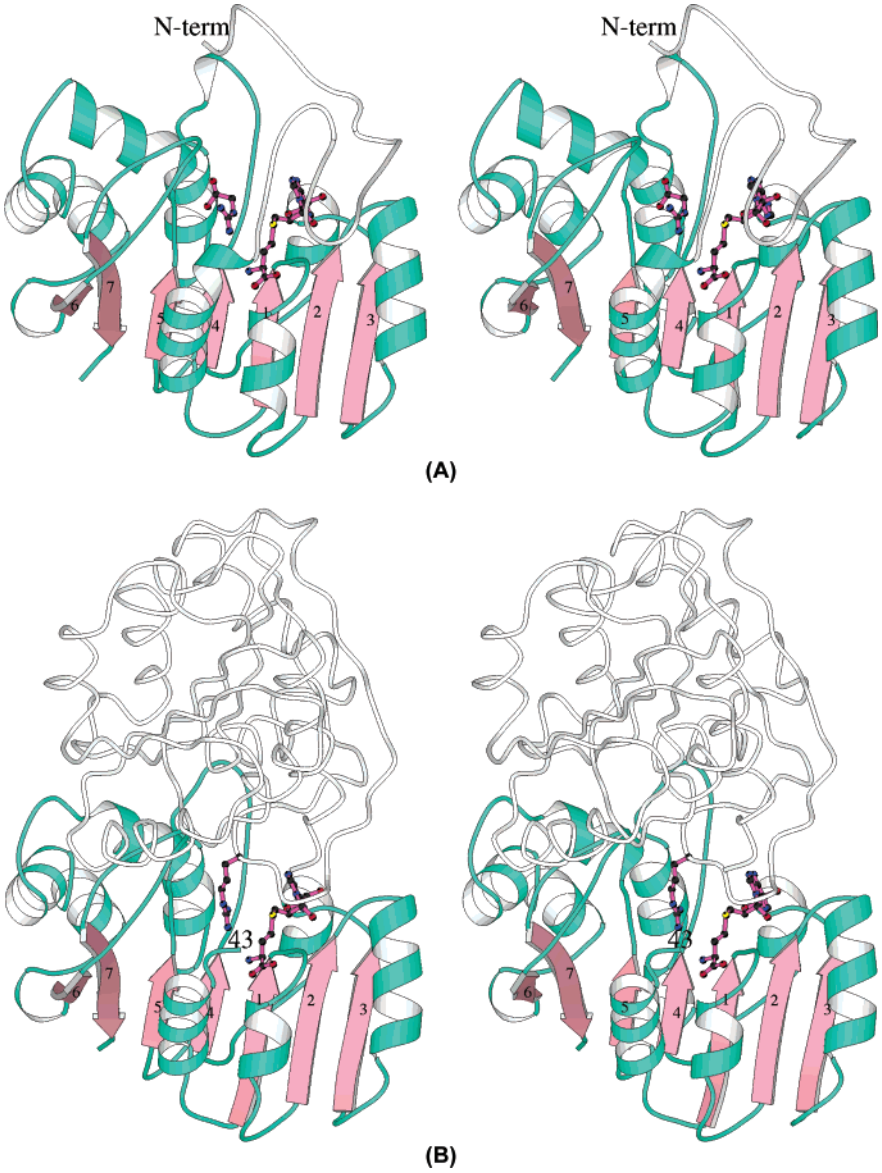


FIGURE 2: (A) A ribbon drawing of the intact GAMT complexed with SAH and GAA (*39*). The N-terminal section (residues 7−42) is illustrated by white coil, which is folded into coil−helix(16−19)−coil−strand(25−26)−coil−strand(33−35)−coil−strand(38−42). The core section (residues 43−235) is shown by aquamarine and light pink. The numbers on the $\beta$-strands are assigned numbers. The bound SAH and GAA are illustrated by ball-and-stick mode. (B) The truncated enzyme that lacks residues 1−36 forms a dimer (two subunits are drawn with ribbon and white coil). R220 of one subunit enters deeply in the active site of the other and forms a pair of H-bonds with D134.

oxygen binding site of GAA. Therefore, the H-bonding networks around GUN are quite similar to those around GAA.

*Model Structure of GAMT Containing SAM and GAA.* The GAMT−(SAM + GAA) model structure was built by attaching a methyl group ($C_E$) to $S_D$ of the bound SAH in GAMT−(SAH + GAA). The $C_E$ position was identified by superimposing SAM in a well-refined structure in the Protein Data Bank [SAM in heat shock protein FtsJ determined at 1.5 Å resolution (*36*) was used] on the bound SAH in GAMT−(SAH + GAA). In this model structure, the distance between $C_E$ of SAM and $N_E$ of GAA ($C_E \cdots N_E$) is 2.2 Å, and the $S_D-C_E \cdots N_E$ bonds are nearly linear. SAM has an *S*-configuration at the $S_D$ atom, which is seen in naturally occurring SAM (*37*, *38*).

*Enzyme Activities of the Mutated Enzymes.* E45 and D134 are involved in H-bonds with the guanidino group of GAA and apparently play important roles in the catalytic reaction. These two residues along with Y221 were mutated, and the catalytic activities of the mutated enzymes were compared with that of WT. As shown in Table 2, the E45S and D134A mutations inactivate the enzymes. The D134N mutations reduce the $k_{cat}$ values significantly, while reduction of $k_{cat}$ values by the E45D, E45Q, D134E, and Y221F mutations is relatively small. Changes in the $K_M$(SAM) and $K_M$(GAA) values caused by the E45D and E45Q mutations are relatively small, whereas the D134N and D134E mutations increase the $K_M$(SAM) and $K_M$(GAA) values significantly. All mutations reduce $k_{cat}/K_M$(SAM). The $k_{cat}/K_M$(GAA) values of E45D and E45Q are at the same level as that of WT, while the other mutations reduce $k_{cat}/K_M$(GAA) significantly. Since E45, D134, and Y221 interact with GAA but not SAM in the crystal structure, the large increases in $K_M$(SAM) are mainly due to a change of either the active site geometry or the hydration degree on the active site surface. The $k_{cat}/K_M$-(GAA) values will be mainly used for discussion because

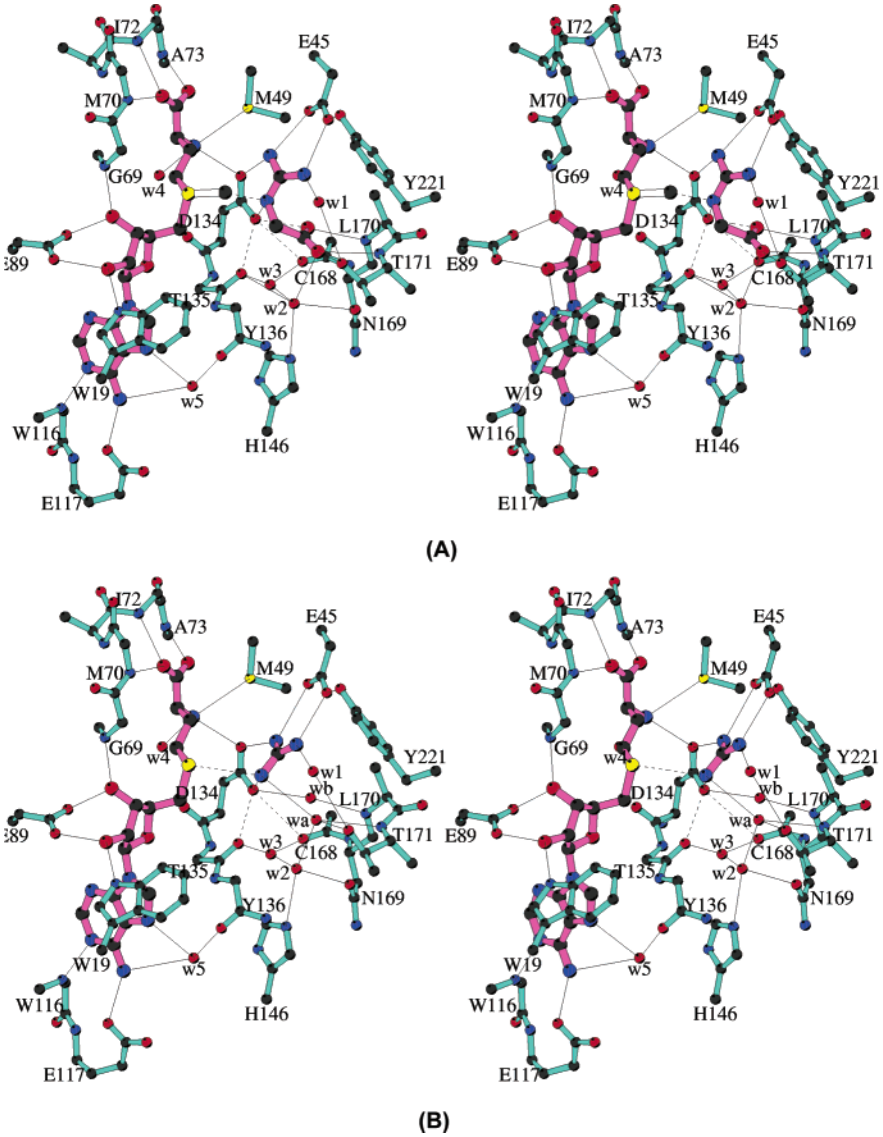


FIGURE 3: H-Bond networks around the bound SAH and GAA in the active site. Possible H-bonds are represented with thin lines, and O···O interactions are represented with dashed lines. The attached methyl group ($C_E$) on SD of SAH has a white bond. The $N_E$···$C_E$ distance between GAA and SAM is 2.2 Å. SAH and GAA/GUN have magenta bonds, while the amino acid residues have aquamarine bonds: (A) GAMT−(SAH + GAA) and (B) GAMT−(SAH + GUN). The H-bonds around SAH have been omitted.

Table 2: Apparent Kinetic Constants of Wild-Type and Variant GAMT

| | | $K_M$ ($\mu$M) | | $k_{cat}/K_M$ | |
|---|---|---|---|---|---|
| enzyme | $k_{cat}$ ($min^{-1}$) | SAM | GAA | SAM[a] | GAA[a] |
| WT | 3.8 ± 0.2 | 2.0 ± 0.1 | (5.0 ± 0.2) × 10 | 1.0 | 1.0 |
| E45D | 2.4 ± 0.1 | 4.2 ± 0.1 | (2.2 ± 0.1) × 10 | $2.9 \times 10^{-1}$ | 1.4 |
| E45Q | 1.0 ± 0.1 | 8.8 ± 0.2 | (1.3 ± 0.1) × 10 | $6.1 \times 10^{-2}$ | 1.0 |
| E45S[b] | 0 | − | − | 0 | 0 |
| D134E[c] | 1.7 ± 0.1 | (1.1 ± 0.1) × $10^3$ | (1.9 ± 0.1) × $10^3$ | $7.8 \times 10^{-4}$ | $1.1 \times 10^{-2}$ |
| D134N[c] | (4.0 ± 0.2) × $10^{-2}$ | (5.7 ± 0.2) × $10^3$ | (1.2 ± 0.1) × $10^3$ | $3.6 \times 10^{-6}$ | $4.3 \times 10^{-4}$ |
| D134A[b,c] | 0 | − | − | 0 | 0 |
| Y221F | 2.1 ± 0.1 | (2.4 ± 0.1) × 10 | (2.3 ± 0.1) × $10^3$ | $4.6 \times 10^{-2}$ | $1.2 \times 10^{-2}$ |

[a] Value relative to that of WT. [b] Inactive. [c] From ref *31*.

mutations of E45, D134, and Y221 are expected to alter these values.

*GUN Is a Weak Inhibitor*. There has been no report about the inhibitor of GAMT except for the general methyltransferase inhibitor SAH. We have examined simple guanidino derivatives (GUN, methyl-GUN, and amino-GUN) to determine whether those compounds are substrates or inhibitors. These GUN derivatives showed a weak inhibitory activity ($IC_{50}$ = 10−100 $\mu$M).

## DISCUSSION

*Differences between the Intact and Truncated Enzymes.* The truncated enzyme that lacks residues 1−36 forms a dimer, in which R220 of one subunit enters deeply the active

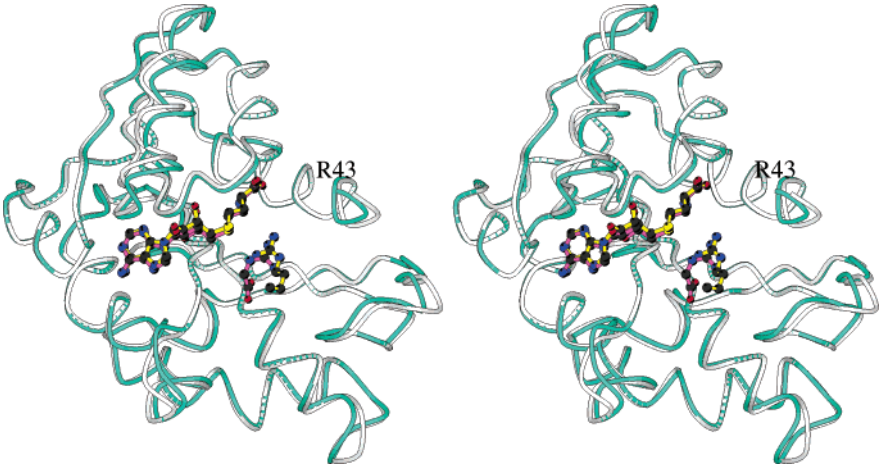


FIGURE 4: Superimposed view of the intact and N-terminally truncated enzymes. The $C_A$ positions of the N-terminally truncated enzyme (residues 43−235) were superimposed on the corresponding $C_A$ positions of the intact enzyme. The N-terminal section (residues 7−42) of the intact enzyme has been omitted for clarity. The intact and truncated enzymes are shown with aquamarine and white coils, respectively. The bound SAH and GAA in the intact enzyme and the bound SAH and R220 in the truncated enzyme are illustrated as magenta and yellow bond models, respectively.

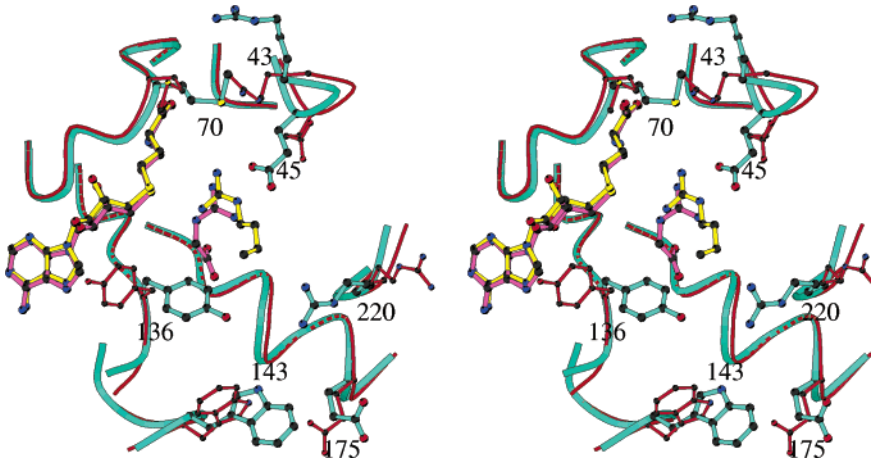


FIGURE 5: Superimposed view of the active sites of the intact and truncated enzymes. The amino acid residues of the intact and truncated enzymes are illustrated with aquamarine and red coils, respectively. The side chains of the truncated enzyme that changed the orientations are shown with red bond models with the residue numbers. The bound SAH and GAA in the intact enzyme and the bound SAH and R220 in the truncated enzyme are illustrated with magenta and yellow bond models, respectively.

site of the other and forms a pair of H-bonds with D134 (Figure 2B). On the other hand, the intact enzyme is a monomer and the polypeptide composed of residues 1−42 covers the active site cleft. As shown in Figure 4, the backbones of the intact and truncated enzymes are superimposable, and the rmsd of $C_A$ positions between the intact and truncated enzymes is 0.7 Å. However, several side chains of the amino acid residues located near the GAA binding site are oriented differently (Figure 5). These are R43, E45, M70, Y136, W143, E175, and R220. When the intact enzyme structure is superimposed on the truncated enzyme structure, there are obvious collisions between residues 7−42 of the intact enzyme and the side chains oriented differently in the truncated enzyme, suggesting that the side chains of these amino acid residues are quite movable if the N-terminal section is moved out to open the active site entrance. Such side chain movements would facilitate release of the product from the active site.

*GAMT Should Have at Least Two Conformations.* As shown in Figure 2A, the active site of the intact GAMT is not visible because the N-terminal section (residues 1−42) covers the active site cleft (closed conformation). For the substrates to enter the active site and to release the products from the active site, the N-terminal section has to move out to open the active site entrance (open conformation). In the closed conformation, there are 14 H-bonds and 7 water-mediated H-bonds between the N-terminal and core sections. The number of H-bonds is relatively small, suggesting that the N-terminal section is readily separated from the core section. For example, the bound SAH and GAA have 14 and 9 H-bonds, respectively. Obviously, when the active site entrance is opened, water molecules can flow into the active site along with the substrates. For the catalytic reaction to occur, it is necessary to exclude unnecessary water molecules from the active site. The role of the N-terminal section could be to exclude water molecules from the active site. Indeed, the N-terminally truncated enzyme has the intact active site but does not have the GAMT catalytic activity.

*Proposed Catalytic Mechanism.* On the basis of the crystal structure of GAMT−(SAH + GAA) and the model structure of GAMT−(SAM + GAA), a possible catalytic mechanism of the methyl transfer reaction of GAMT is proposed. Brownian motion moves the N-terminal section to open the active site entrance. SAM and GAA molecules enter and

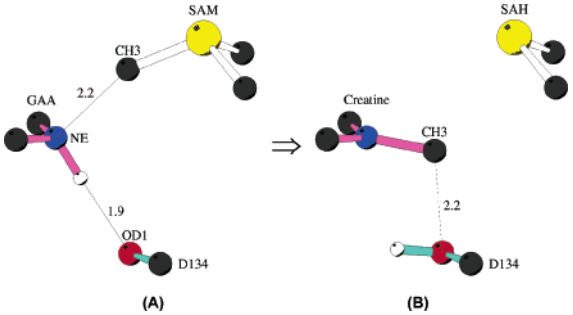


FIGURE 6: Diagram showing the pre- and post-methyl transfer reaction of GAMT. (A) $O_{D1}$[D134] and $CH_3$[SAM] approach $N_E$ of GAA from the tetrahedral directions. (B) The methylated $N_E$ goes back to the $sp^2$ hybridization so that the bulky methyl group breaks a pair of H-bonds with D134. Thin and dashed lines represent a H-bond and a short contact, respectively. The numbers indicate the C···N, O···H, and C···O distances (in angstroms).

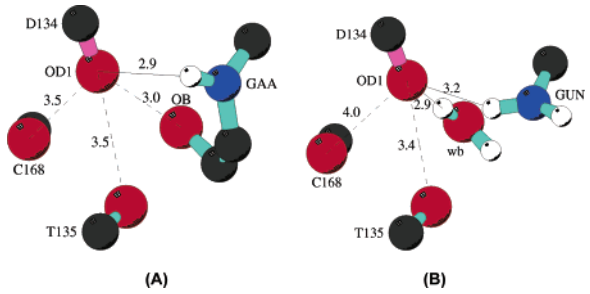


FIGURE 7: Diagram showing two different types of environment around $O_{D1}$[D134]: (A) higher-p$K_a$ environment seen in GAMT−(SAH + GAA) and (B) lower-p$K_a$ environment seen in GAMT−(SAH + GUN). Thin and dashed lines represent a H-bond and a short contact, respectively. The numbers indicate the C···N, O···N, and C···O distances (in angstroms).

bind to the SAM and GAA binding sites, respectively, as seen in the crystal structure. SAM and GAA are firmly attached in the active site by H-bonds (Figure 3A). The N-terminal section moves back to the closed conformation position, and thus, unbound water molecules are excluded from the active site. There are two characteristic features at this stage.

(1) $O_{D1}$[D134] and $C_E$[SAM] approach $N_E$ of GAA from the tetrahedral directions. The $N_E$···$O_{D1}$ and $N_E$···$C_E$ distances are 2.9 and 2.2 Å, respectively, and the $S_D$−$C_E$···$N_E$ bonds are nearly linear (Figure 6A).

(2) $O_{D1}$ of D134 forms a H-bond with $N_E$ of GAA and is surrounded by three slightly negatively charged carbonyl oxygens ($O_B$[GAA], O[T135], and O[C168]), all within 3.5 Å (Figure 7A). In this environment, the p$K_a$ value of $O_{D1}$ should be relatively high.

As illustrated in Figure 8, the following events occur.

(1) The negatively charged $O_{D1}$ of D134 interacts with the hydrogen attached to $N_E$ of GAA so that the hydrogen is displaced from the $sp^2$ hybridization plane and is tilted toward the oxygen (Figure 6A). The electron configuration at $N_E$ then approaches $sp^3$ hybridization, and the lone pair electrons are pointed toward the $C_E$ atom of SAM. Since the $O_{D1}$ environment increases the p$K_a$ value, $O_{D1}$ abstracts the proton on $N_E$ of GAA. The deprotonated $N_E$ of GAA could be a strong nucleophile, which abstracts the methyl group ($C_E$) on the positively charged $S_D$ of SAM. Specifically, a pair of electrons shift from $O_{D1}^-$ of D134 to $S_D^+$ of SAM as illustrated in Figure 8. The H−$O_{D1}$ and $N_Z$−$C_E$ bonds are formed, while the $N_Z$−H and $C_E$−$S_D$ bonds are cleaved. The methyl group of SAM is transferred to $N_E$ of GAA by an $S_N2$ reaction mechanism.

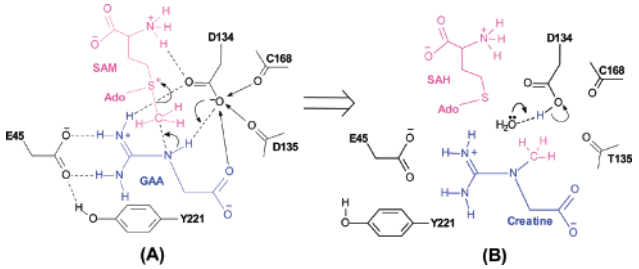


FIGURE 8: Proposed mechanism of the methyl transfer reaction of GAMT. (A) Transition stage in which $N_E$ of GAA has $sp^3$ hybridization. The three slightly negatively charged carbonyl oxygens (O of T135, O of C168, and $O_B$ of GAA) increase the p$K_a$ value of $O_{D1}$ so that $O_{D1}$ abstracts the proton on $N_E$ of GAA. A strong nucleophile is generated on the deprotonated $N_E$ of GAA, which abstracts the methyl group ($C_E$) from the positively charged $S_D$ of SAM. E45 and Y221 participate in building the active site framework. (B) Postreaction stage. The methylated $N_E$ goes back to the $sp^2$ hybridization so that the bulky methyl group breaks a pair of H-bonds with D134, and the products creatine and then SAH are released from the active site. A water molecule occupies the $O_B$ binding site; $O_{D1}$ releases the proton, and the p$K_a$ value goes back to a normal level. Curved arrows denote the movements of electron pairs. Possible polar interactions are illustrated with dashed lines. The plus and minus signs indicate positive and negative charge, respectively. Straight arrows denote O···O interactions between three carbonyl oxygens (O[T135], O[C168], and $O_B$[GAA]) and $O_{D1}$[D134].

(2) Since the methylated $N_E$ goes back to the $sp^2$ hybridization, the product creatine breaks a pair of H-bonds with D134 and is released from the active site (Figure 6B). Brownian motion moves the N-terminal section to open the active site entrance, and the product creatine followed by the demethylated SAM (SAH) leaves the active site. D134 releases a proton to solvent because its p$K_a$ value decreases to normal.

*The E45, D134, and Y221 Mutation Data Support the Proposed Mechanism.* Since E45 and D134 participate in a pair of H-bonds with the guanidino group of GAA, mutations of these residues are expected to affect the catalytic activity. As shown in Table 2, the E45S, D134N, and D134A mutations reduce the $k_{cat}$ values drastically. As will be described below, the E45S mutation would induce conformational changes in the active site, and subsequently, the substrate binding is inhibited. In the proposed catalytic mechanism, D134 participates not only in the substrate binding but also in the catalytic reaction as a general base. Since the D134A and D134N mutant enzymes cannot abstract the proton on $N_E$ of GAA, the $k_{cat}$ values are reduced drastically. The D134E mutation should increase $K_M$(GAA) because it would disrupt the GAA binding by changing the active site surface. However, since the D134E mutant enzyme could abstract the proton on $N_E$ of GAA, it has a considerably large $k_{cat}$ value.

Interestingly, the conservative mutations (E45Q and E45D) of E45 do not reduce the $k_{cat}$ and $k_{cat}/K_M$(GAA) values drastically, but a nonconservative mutation (E45S) inactivates the enzyme. Since in the crystal structure the guanidino group of GAA is bound to the enzyme firmly by five H-bonds, it might not be critical for substrate binding if one or two H-bonds are broken. Indeed, E45 does not form a pair of

H-bonds with the guanidino group of Arg220 in the truncated structure. Therefore, it is reasonable to expect that the E45Q and E45D mutant enzymes retain their considerable catalytic activity.

There must be a completely different reason for the fact that the E45S mutation abolishes catalytic activity. The carboxylate group of E45 forms a H-bond with OH of Y221 in the crystal structures of the intact and truncated enzymes. The hydroxyphenyl group of Y221 is located on the active site surface and appears to be a wall of the active site. When E45 is replaced with a short side chain Ser, the H-bond connecting to the two residues is no longer present. The hydroxyphenyl group of Y221 could move freely, move into the GAA binding site, and prevent the GAA binding. To prove this hypothesis, the Y221F mutant enzyme was made, and the catalytic activity was determined. As expected, the Y221F mutation increases $K_M$ by 500-fold but does not affect $k_{cat}$. Therefore, E45 and Y221 appear to have structural roles in building the active site framework.

*Why Is GUN Not a Substrate of GAMT?* Since GUN binds at the same site of the guanidino group of GAA in the crystal structure, GUN can be a substrate of GAMT and receive a methyl group from SAM. However, GUN, methyl-GUN, and amino-GUN are all weak inhibitors of GAMT. In the proposed catalytic mechanism, the p$K_a$ value of $O_{D1}$[D134] is increased by the slightly negatively charged carbonyl oxygens (O[T135], O[C168], and $O_B$[GAA]), and thus, it can abstract the proton on $N_E$ of GAA. In an inhibitor complex [GAMT−(SAH + GUN)], $O_{D1}$[D134] is surrounded by two carbonyl oxygens (O[T135] and O[C168]) and a water molecule ($w_b$) located at the $O_B$ binding site of the GAA carboxylate (Figures 3B and 7B). $O_{D1}$ forms a H-bond with the water molecule. In this environment, the p$K_a$ value of $O_{D1}$ would not be high enough to abstract the proton on $N_E$ of GUN. Therefore, GUN is an inhibitor but not a substrate. Similarly, methyl-GUN and amino-GUN bind at the same site of GUN and inhibit GAA binding. It is noted that such a water molecule ($w_b$) is not observed in the N-terminally truncated enzyme structure.

The inhibitory activity of simple guanidine analogues supports the proposed mechanism in which the p$K_a$ value of $O_{D1}$[D134] is increased by $O_B$[GAA]. However, it is necessary to prove that carbonyl groups of both T135 and C168 are involved in the $O_{D1}$[D134] activation. As shown in Figure 7A, $O_{D1}$[D134] sits on three oxygen atoms (O[T135], O[C168], and $O_B$[GAA]). If one of the carbonyl oxygen sites were empty, $O_{D1}$ would be shifted toward the empty site to prevent the charge−charge repulsion from $O_B$[GAA] and the other carbonyl oxygen. In the higher-p$K_a$ environment (Figure 7A), the two carbonyl oxygens are within 3.5 Å of $O_{D1}$. On the other hand, O[C168] moves away from $O_{D1}$ in the lower-p$K_a$ environment (Figure 7B). The differences in environment around $O_{D1}$[D134] in GAMT−(SAH + GAA) and GAMT−(SAH + GUN) suggest that two carbonyl oxygens adjacent to $O_{D1}$[D134] are essential to increasing the p$K_a$ value of $O_{D1}$.

Mutation of T135 or C168 might alter the position of the invoked carbonyl enough to prove that indeed T135 or C168 is important for the early stage of the mechanism. However, since the conformation changes in the main chain must alter the positions of side chains, it would be difficult to obtain conclusive evidence by a mutagenesis approach.

## ACKNOWLEDGMENT

We thank Professors Richard H. Himes for a critical reading of the manuscript and very valuable comments.

## REFERENCES

1. Cantoni, G. L., and Vignos, P. J., Jr. (1954) Enzymatic mechanism of creatine synthesis, *J. Biol. Chem. 209*, 647−659.
2. Mudd, S. H., and Poole, J. R. (1975) Labile methyl balances for normal humans on various dietary regimens, *Metabolism 24*, 721−735.
3. Mudd, S. H., Ebert, M. H., and Scriver, C. R. (1980) Labile methyl group balances in the human: the role of sarcosine, *Metabolism 29*, 707−720.
4. Hurwitz, J., Gold, M., and Anders, M. (1964) The enzymatic methylation of ribonucleic acid and deoxyribonucleic acid. IV The properties of the soluble ribonucleic acid-methylating enzymes, *J. Biol. Chem. 239*, 3474−3482.
5. Deguchi, T., and Barchas, J. (1971) Inhibition of transmethylations of biogenic amines by *S*-adenosylhomocysteine. Enhancement of transmethylation by adenosylhomocysteinase, *J. Biol. Chem. 246*, 3175−3181.
6. Coward, J. K., Slixz, E. P., and Wu, F. Y. (1973) Kinetic studies on catechol *O*-methyltransferase. Product inhibition and the nature of the catechol binding site, *Biochemistry 12*, 2291−2297.
7. Pugh, C. S., Borchardt, R. T., and Stone, H. O. (1977) Inhibition of Newcastle disease virion messenger RNA (guanine-7-)-methyltransferase by analogues of *S*-adenosylhomocysteine, *Biochemistry 16*, 3928−3932.
8. Hasobe, M., Mckee, J. G., and Borchardt, R. T. (1989) Relationship between intracellular concentration of *S*-adenosylhomocysteine and inhibition of vaccinia virus replication and inhibition of murine L-929 cell growth, *Antimicrob. Agents Chemother. 33*, 828−834.
9. Stöckler, S., Holzbach, U., Hanefeld, F., Marquardt, I., Helms, G., Requart, M., Hänicke, W., and Frahm, J. (1994) Creatine deficency in the brain: a new, treatable inborn error of metabolism, *Pediatr. Res. 36*, 409−413.
10. Stöckler, S., Isbrandt, D., Hanefeld, F., Schmidt, B., and von Figura, K. (1996) Guanidinoacetate methyltransferase deficiency: the first inborn error of creatine metabolism in man, *Am. J. Hum. Genet. 58*, 914−922.
11. Stöckler, S., Marescau, B., De Deyn, P. P., Trijbels, J. M., and Hanefeld, F. (1997) Guanidino compounds in guanidinoacetate methyltransferase deficiency, a new inborn error of creatine synthesis, *Metabolism 46*, 1189−1193.
12. von Figura, K., Hanefeld, F., Isbrandt, D., and Stockler-Ipsiroglu, S. (2000) Guanidinoacetate methyltransferase deficiency, in *The metabolic and molecular basis of inherited disease* (Scrver, C. R., Beaudet, A., Sly, W. S., and Valle, D., Eds.) pp 1897−1908, McGraw-Hill, New York.
13. Schulze, A., Ebinger, F., Rating, D., and Mayatepek, E. (2001) Improving treatment of guanidinoacetate methyltransferase deficiency: reduction of guanidinoacetic acid in body fluids by arginine restriction and ornithine supplementation, *Mol. Genet. Metab. 74*, 413−419.
14. Im, Y. S., Cantoni, G. L., and Chiang, P. K. (1979) A radioactive assay for guanidinoacetate methyltransferase, *Anal. Biochem. 95*, 87−88.
15. Ogawa, H., Ishiguro, Y., and Fujioka, M. (1983) Guanidinoacetate methyltransferase from rat liver: purification, properties, and evidence for the involvement of sulfhydryl groups for activity, *Arch. Biochem. Biophys. 226*, 265−275.
16. Ogawa, H., Date, T., Gomi, T., Konishi, K., Pitot, H. C., Cantoni, G. L., and Fujioka, M. (1988) Molecular cloning, sequence analysis, and expression in *Escherichia coli* of the cDNA for guanidinoacetate methyltransferase from rat liver, *Proc. Natl. Acad. Sci. U.S.A., 85*, 694−698.
17. Isbrandt, D., and von Figura, K. (1995) Cloning and sequence analysis of human guanidinoacetate *N*-methyltransferase cDNA, *Biochim. Biophys. Acta 1264*, 265−267.
18. Fujioka, M., Konishi, K., and Takata, Y. (1988) Recombinant rat liver guanidinoacetate methyltransferase: reactivity and function of sulfhydryl groups, *Biochemistry 27*, 7658−7664.
19. Fujioka, M., Takata, Y., and Gomi, T. (1991) Recombinant rat guanidinoacetate methyltransferase: structure and function of the

$NH_2$-terminal region as deduced by limited proteolysis, *Arch. Biochem. Biophys. 285*, 181−186.
20. Takata, Y., and Fujioka, M. (1990) Recombinant rat liver guanidinoacetate methyltransferase, *Int. J. Biochem. 22*, 1333−1339.
21. Takata, Y., Date, T., and Fujioka, M. (1991) Rat liver guanidinoacetate methyltransferase: proximity of cycteine residues at position 15, 90 and 219 as revealed by site-directed mutagenesis and chemical modification, *Biochem. J. 277*, 399−409.
22. Takata, Y., and Fujioka, M. (1992) Identification of a tyrosine residue in rat guanidinoacetate methyltransferase that is photolabeled with *S*-adenosyl-L-methionine, *Biochemistry 31*, 4369−4374.
23. Takata, Y., Konishi, K., Gomi, T., and Fujioka, M. (1994) Rat guanidinoacetate methyltransferase. Effect of site directed alteration of an aspartic acid residue that is conserved across most mammalian *S*-adenosylmethionine-dependent methyltransferases, *J. Biol. Chem. 269*, 5537−5542.
24. Komoto, J., Huang, Y., Takata, Y., Yamada, T., Konishi, K., Ogawa, H., Gomi, T., Fujioka, M., and Takusagawa, F. (2002) Crystal structure of guanidinoacetate methyltransferase from rat liver: a model structure of protein arginine methyltransferase, *J. Mol. Biol. 320*, 223−235.
25. Komoto, J., Takata, Y., Yamada, T., Konishi, K., Ogawa, H., Gomi, T., Fujioka, M., and Takusagawa, F. (2003) Monoclinic guanidinoacetate methyltransferase and gadolinium ion-binding characteristics, *Acta Crystallogr. D59*, 1589−1596.
26. Stultz, C. M., White, J. V., and Smith, T. F. (1993) Structural analysis based on state-space modeling, *Protein Sci. 2*, 305−314.
27. Komoto, J., Huang, Y., Hu, Y., Takata, Y., Konishi, K., Ogawa, H., Gomi, T., Fujioka, M., and Takusagawa, F. (1999) Crystallization and preliminary X-ray diffraction studies of guanidinoacetate methyltransferase from rat liver, *Acta Crystallogr. D55*, 1928−1929.
28. Otwinowski, Z., and Minor, W. (1997) Processing of X-ray Diffraction Data Collected in Oscillation Mode, *Methods Enzymol. 276*, 307−326.
29. Brünger, A. T. (1993) *X-PLOR 3.82: A system for X-ray crystallography and NMR*, Yale University Press, New Haven, CT.
30. Kunkel, T. A., Roberts, J. D., and Zakour, R. A. (1987) Rapid and efficient site-specific mutagenesis without phenotypic selection, *Methods Enzymol. 154*, 367−382.
31. Sanger, F., Nicklen, S., and Coulson, A. R. (1977) DNA sequencing with chain-terminating inhibitors, *Proc. Natl. Acad. Sci. U.S.A. 74*, 5463−5467.
32. Laskowski, R. A., MacArthur, M. W., Moss, D. S., and Thornton, J. M. (1993) PROCHECK: A program to check the stereochemical quality of protein structures, *J. Appl. Crystallogr. 26*, 283−291.
33. Kagan, R. M., and Clarke, S. (1994) Widespread occurrence of three sequence motifs in diverse S-adenosylmethionine-dependent methyltransferases suggests a common structure for these enzymes, *Arch. Biochem. Biophys. 310*, 417−427.
34. Hamahata, A., Takata, Y., Gomi, T., and Fujioka, M. (1996) Probing the *S*-adenosylmethionine-binding site of rat guanidinoacetate methyltransferase. Effect of site-directed mutagenesis of residues that are conserved across mammalian non-nucleic acid methyltransferases, *Biochem. J. 317*, 141−145.
35. Gomi, T., Tanihara, K., Date, T., and Fujioka, M. (1992) Rat guanidinoacetate methyltransferase: mutation of amino acids within a common sequence motif of mammalian methyltransferase does not affect catalytic activity but alters proteolytic susceptibility, *Int. J. Biochem. 24*, 1639−1649.
36. Bugl, H., Fauman, E. B., Staker, B. L., Zheng, F., Kushner, S. R., Saper, M. A., Bardwell, J. C., and Jakob, U. (2000) RNA methylation under heat shock control, *Mol. Cell 6*, 349−360.
37. Cornforth, J. W., Reichard, S. A., Talalay, P., Carrell, H. L., and Glusker, J. P. (1977) Determination of the absolute configuration at the sulfonium center of *S*-adenosylmethionine. Correlation with the absolute configuration of the diastereomeric *S*-carboxymethyl-(*S*)-methionine salts, *J. Am. Chem. Soc. 99*, 7292−7300.
38. Stolowitz, M. L., and Minch, M. J. (1981) *S*-Adenosyl-L-methionine and *S*-adenosyl-L-homocysteine, an NMR study, *J. Am. Chem. Soc. 103*, 6015−6019.
39. Kraulis, P. J. (1991) MOLSCRIPT: A program to produce both detailed and schematic plots of protein structures, *J. Appl. Crystallogr. 24*, 946−950.

BI0486785